[논문] 태양에너지
Solar Energy
Vol. 18, No. 3, 1998

Review of Entrainment and Interfacial Stability in Thermosyphons and Capillary-Driven Heat Pipes

B. H. Kim*, C. J. Kim**

* *Taegu University*

** *Sung Kyun Kwan University*

ABSTRACT

Entrainment in thermosyphons and heat pipes was characterized in view of the interfacial stability associated with the critical Weber number and the entrainment limit at the onset of liquid entrainment from the liquid or wicked interface. Both literature review and theoretical analysis on the entrainment models were performed in order to evaluate accuracy of the predicted value.

For this purpose, the models were categorized in two groups according to their entrainment mechanism and interfacial configurations, i.e., the wave-induced entrainment and the shear-induced entrainment, respectively. Thus, the twelve models (five models for the wave-induced entrainment and seven for the shear induced entrainment) were examined to obtain individual trends and their discrepancies from the general tendency of the overall models. As a result, the critical Weber numbers and entrainment limits were calculated and represented as a function of vapor temperature for the chosen characteristic dimensions of the interface.

NOMENCLATURE

c_k empirical constants
d_1 wire spacing(m)
d_2 wire thickness(m)
$d_{h,w}$ hydraulic diameter of a wick pore(m)
D_h duct hydraulic diameter or vapor core diameter(m)
E_1^* entrainment number
f_u f_{vi} liquid and vapor friction factor at the interface
g gravitational acceleration(m/s^2)
h film thickness(m) or enthalpy(J/kg)
h_{fg} latent heat of vaporization(J/kg)
L characteristic wick dimension(m)
q heat transport(W)
Q_c^* dimensionless entrainment limit
t time(s)
U mean vapor velocity(m/s)
v^+ dimensionless vapor velocity
vc critical mean velocity(m/s)
e Weber number

INTRODUCTION

When the relative velocity between the vapor and liquid is sufficiently large, the interface becomes unstable and the destabilizing effect appears in the form of a wave at the interface. As the velocity increases, the enhanced wave action, together with the viscous shear forces occurring at the liquid/vapor interface may inhibit the return of liquid to the evaporator. When this occurs, the heat pipe or the liquid-vapor flow system is said to have reached the flooding limit (Kutateladze and Sorokin, 1969 ; Dobran, 1985).

With further increases in the velocity, the interfacial shear force may become sufficient to overcome the liquid surface-tension force and cause liquid droplets to be stripped or torn off the wavy liquid/vapor interface and entrained into the vapor flow. This entrainment of liquid droplets leads to partial or total dry-out and limits the axial heat transport. This phenomenon is referred to as the entrainment limit(Tien and Chung, 1979; Ivanovskii et al., 1982 ; Prenger, 1984).

Shortly after the invention of the heat pipe by Grover et al.(1964), numerous approaches to predict the onset of entrainment were established using the instability criterion of Kelvin(1871) derived from the Kelvin-Helmholtz instability theories or the empirical flooding correlations proposed by Wallis(1969) and Kutateladze and Sorokin(1969). Later, Tien and Chung(1979) presented a semi-empirical criterion to predict the entrainment limit for various types of heat pipes by incorporating the characteristic wavelength of the capillary flow into the flooding correlations. In addition, Ishii and Grolmes(1975) proposed the roll-wave entrainment model based upon the roll-wave geometry commonly observed in two-phase internal flows.

THEORETICAL BACKGROUND

In the two groups of entrainment models, the wave-induced entrainment occurs when

the wick structure is fully flooded. The instability criterion(Kelvin, 1871 ; Drazin and Reid, 1981 ; Carey, 1992), the modified flooding correlation for non-wicked heat pipes(Tien and Chung, 1979) and the roll-wave model (Ishii and Grolmes, 1975) can be included in this category. The shear-induced entrainment results from the shear forces induced by high velocity vapor flows when the wick structure is properly saturated. Several analytical models such as the Weber number criterion (Chi, 1976), the instability criterion(Cotter, 1967) and the entrainment limit criterion derived from flooding correlations (Tien and Chung, 1979) were investigated to predict the entrainment limit in wicked heat pipes.

For the critical velocity models such as the Weber number criterion(Chi, 1976) and the instability criterion(Cotter, 1967), the entrainment limit can be estimated using an energy balance equation,

$$q_e = \rho_v A_v h_{fg} U_{vc} \tag{1}$$

Wave-Induced Entrainment

When the wick structure is flooded due to the overcharge of working fluid or increased vapor velocity, the instability criterion (Kelvin, 1871) from Kelvin-Helmholtz instability theories, the flooding correlations(Wallis, 1969 ; Kutateladze and Sorokin, 1969 ; Tien and Chung, 1979) and the roll-wave entrainment model(Ishii and Grolmes, 1975) can be utilized to predict critical velocities.

1) Instability Criterion for the Free Interface

In reality, the physical mechanisms for entrainment and unstable wave generation are slightly different, but the wave instability theories can be regarded as a lower bound for the prediction of entrainment onset air/vapor velocity since entrainment is a subsequent phenomenon to the onset of unstable waves.

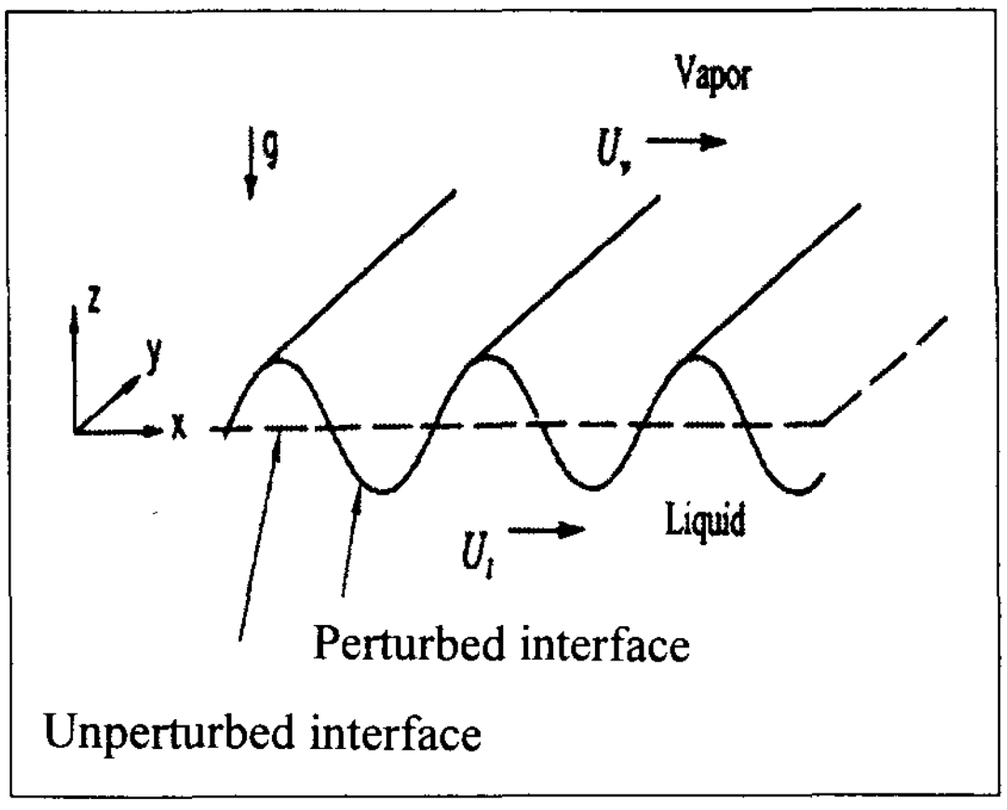

Fig. 1. Configuration of perturbed interface in linear analysis of the inviscid Kelvin-Helmholtz instability(Carey, 1992)

For the ideal case of inviscid Kelvin-Helmholtz type instability, the interface between the two phases can be assumed to be a flat horizontal plane at $z = 0$, as illustrated in Fig. 1. The critical air/vapor velocity is derived as

$$U_{vc} = \left\{\frac{2(\rho_l + \rho_v)}{\rho_l}\right\}^{1/2} \left\{\frac{\sigma(\rho_l + \rho_v)g}{\rho_v^2}\right\}^{1/4} \tag{2}$$

2) Entrainment Limit Criterion Derived from Flooding Correlations

Tien and Chung(1979) modified the Kutateladze flooding correlation by means of the analogy between the entrainment phenomenon in heat pipes and the flooding phenomenon in counterflowing liquid/vapor flow system and proposed a flooding

correlation by recognizing the absence of gravity (i.e., for a horizontal heat pipe) and the presence of capillary structure characterized by h. The corresponding critical heat transport is expressed as

$$q_e = c_k^2 A_l h_{fg} (\sigma/h)^{1/2} (\rho_l^{-1/4} + \rho_v^{-1/4})^{-2} \quad (3)$$

where is the total cross-sectional area of the flow passage.

Prenger (1984) developed a physical model to predict flooding in gravity-assisted heat pipes by means of both a force balance and stability analysis at the interface, as shown in Fig. 2.

An entrainment criterion can be expressed in dimensionless form using a dimensionless heat flux Q_e^* and an entrainment number E_t^*, which were introduced by

$$Q_e^* = \sqrt{2\pi}\, E_t^{*1/2} \quad (4)$$

where Q_e^* is defined as

$$Q_e^* = \frac{q}{\rho_v A_v U_v h_{fg}} = \frac{\rho}{\rho_v A_v h_{fg}^{3/2}} \quad (5)$$

and

$$E_t^* = \frac{q}{\rho_v U_v^2 h} = \frac{\rho}{\rho_v h_{fg} h} \quad (6)$$

3) Roll-Wave Entrainment Model

Ishii and Grolmes(1975) proposed the roll-wave entrainment model based upon the roll-wave geometry commonly observed in the flooding situation of two-phase internal flows, as shown in Fig. 3. The final form of the inception criterion in the transition regime was proposed by Ishii and Grolmes (1975) as

$$j_v^+ \geq 11.78 N_{vi}^{0.8} Re_l^{-1/3} \quad \text{for } N_{vi} \leq 1/15 \quad (7)$$

$$j_v^+ \geq 1.35 Re_l^{-1/3} \quad \text{for } N_{vi} \leq 1/15 \quad (8)$$

For the range where the film Reynolds number exceeds about 1500 to 1750, the film flow becomes completely rough turbulent and the dependence of the liquid friction factor f_{li} on Re_l diminishes. Assuming a critical

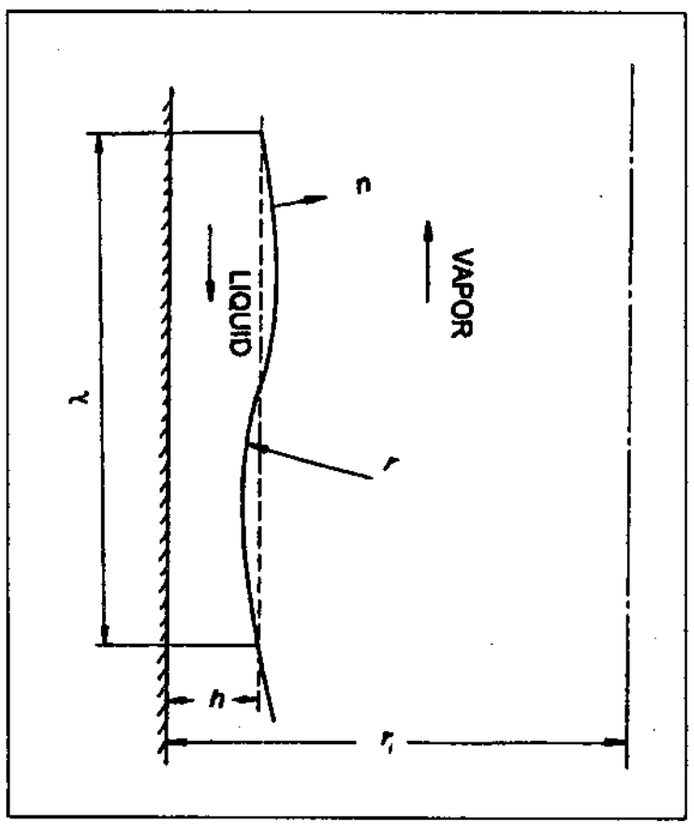

Fig. 2. Configuration of the liquid/vapor interface in vertical counter current flows(Prenger, 1984)

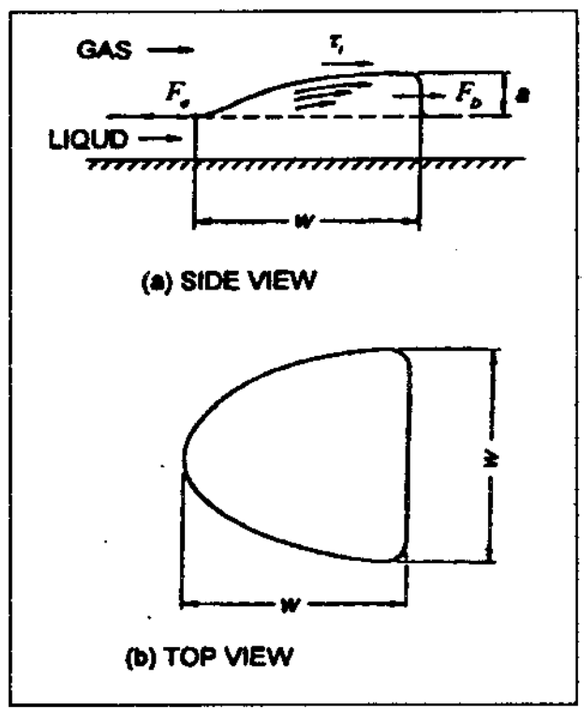

Fig. 3. Force balance on a roll-wave segment; from Ishii and Grolmes(1975), (a) side view, (b) top view

Reynolds number of 1635, Ishii and Grolmes (1975) proposed an inception criterion for the rough turbulent regime as

$$v^{+} = N_{vi}^{0.8} \quad \text{for} \quad N_{vi} < 1/15 \tag{9}$$

$$v^{+} \geq 0.1146 \quad \text{for} \quad N_{vi} > 1/15 \tag{10}$$

Shear-Induced Entrainment

As the vapor velocity increases, the surplus liquid above the wicking structure is carried downstream by a wave propagation or liquid entrainment into the vapor stream. Once the wicked surface is exposed to the vapor stream, the unstable liquid interface tends to be stabilized by the periodic interruption of the capillary structure. In this sense, Busse and Kemme(1980) have expressed doubt as to whether entrainment actually occurs in a capillary-driven heat pipe, since the capillary structure would most likely retard the growth of any surface waves. However, for wavelengths, λ, which are small compared to the hydraulic diameter of a wick pore, $d_{h,w}$, Busse and Kemme(1980) recognized that the damping effect of the capillary structure disappears and entrainment may become possible.

As a first attempt to predict the entrainment limitation in an operating heat pipes, Cotter(1967) applied the hydrodynamic instability concept to horizontal wicked heat pipes and derived an expression for the critical wavelength in terms of the air/vapor velocity. By assuming $g = 0$ and $\rho_l \gg \rho_v$ in equation (2), an expression for the critical air/vapor velocity can be obtained as

$$U_{vc} = \left(\frac{2\pi\sigma}{\rho_v \lambda_c}\right) \tag{11}$$

Equation (11) was experimentally verified using an air-water test channel by Matveev et al. (1977) and Kim et al. (1993). The heat transport corresponding to this critical velocity can be determined by means of the energy balance given in equation (1),

$$q_e = A_v h_{fg} \left(\frac{2\pi\rho_v \sigma}{L}\right)^{1/2} \tag{12}$$

Kemme(1976) proposed a model to predict the entrainment limit for gravity-assisted sodium heat pipes using screen wicks by including a buoyancy force term in the entrainment equation derived by Cotter(1967).

$$q_e = A_v h_{fg} \left\{\frac{\rho_v}{\Omega}\left(\frac{2\pi\sigma}{\lambda} + \rho_l g D_h\right)\right\}^{1/2} \tag{13}$$

where is a turbulent flow factor, which varies from 1.11 to 1.234 for the laminar flow regime (Busse, 1973) and is 2.2 for turbulent flow regime (Olson and Eckert, 1966). For the wavelength, λ, associated with the liquid interface, Kemme(1976) used a slightly different characteristic dimension, the wire spacing plus the diameter of the wires. If the buoyancy force term in equation(13) is neglected, this model appears to be similar to Cotter's original equation except for the flow factor.

Chi(1976) presented a method to predict the entrainment limit for capillary-wicked heat pipes by means of a force balance similar to that presented by Ishii and Grolmes (1975) as

$$e = \frac{1}{E_t^*} = \frac{\rho_v U_v^2 d_{h,w}}{\sigma} \tag{14}$$

The maximum heat transport based upon the critical velocity can be determined using the energy balance given in equation(1).

$$q_e = A_v h_{fg} \left(\frac{\rho_v \sigma}{d_{h,w}} \right)^{1/2} \quad (15)$$

As noted earlier, Tien and Chung(1979) proposed an entrainment limit equation for horizontal non-wicked heat pipes, presented in equation(3). By means of the same analogy used by Cotter(1967) and Kemme(1976), equation(3) can be applied to the entrainment limit for the horizontal wicked heat pipes by replacing the characteristic dimension of the film flow, h, with the characteristic dimension of the capillary structure, L.

$$q_e = c_k^2 A_v h_{fg} (\rho/L)^{1/2} (\rho_l^{-1/4} + \rho_v^{-1/4})^{-2} \quad (16)$$

Prenger and Kemme(1981) performed experiments using gravity-assisted heat pipes with screen wicks, and a semi-empirical model was proposed by correlating the theoretical model obtained from the force balance with the experimental data investigated. The model assumes that a uniform liquid layer is formed along the circumference of the wicking structure and the liquid is returned axially along the heat pipe, as shown in Fig. 4. Finally, the semi-empirical correlation becomes

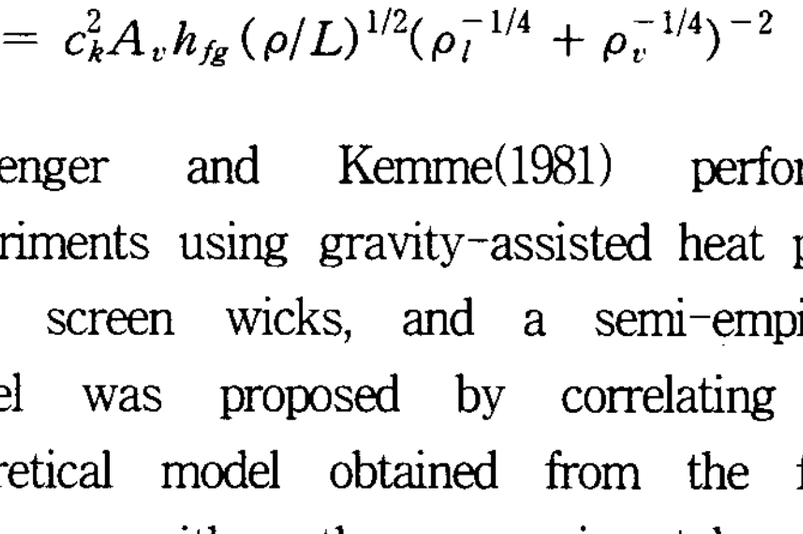

Fig. 4. Force balance on the liquid layer (Prenger and Kemme, 1981)

$$Q_e^* = \sqrt{2\pi/\Omega}\, E_t^{*1/2}\, \delta/\delta^* \quad (17)$$

If equals unity, this equation is identical to the Kemme's criterion(without $\rho_l g D_h$) presented in equation(13).

As noted earlier in equation (29), Prenger (1984) developed a theoretical model to predict flooding in gravity-assisted heat pipes.

$$U_l = \left(\frac{\sigma}{\rho_l \delta} \right)^{1/2} \quad (18)$$

where δ represents the characteristic dimension of the wicking structure as presented by Prenger and Kemme(1981). By means of mass and energy conservation, the heat transport can be expressed in terms of a dimensionless entrainment criterion can be obtained as

$$Q_e^* = 4 \frac{\delta}{D_h} \left(\frac{\rho_l}{\rho_v} \right)^{1/2} E_t^{*1/2} \quad (19)$$

Another approach to predict the entrainment limit for heat pipes with fine meshes was proposed by Rice and Fulford (1987), who assumed that the only pressure difference(ΔP) between the liquid in the mesh and the vapor is the kinetic head of the flow. The critical heat transport corresponding to this vapor velocity can be determined from an energy balance equation.

$$q_e = A_v h_{fg} \left(\frac{8 \sigma \rho_v}{d_1} \right)^{1/2} \quad (20)$$

SUMMARY OF MODEL COMPARISON

As shown in Table 1, twelve models(five models for the wave-induced entrainment and seven for the shear-induced entrainment) were examined to determine the individual trends and deviation from the general tendency of the overall models. For this purpose, critical Weber numbers and entrainment limits were calculated for the chosen characteristic dimensions of the interface and working fluid (water).

Table 1. Summary of various models

Groups	Models	σ	ρ_v	ρ_l	μ	λ
Wave-induced	Kelvin(1871) : Eq.(2)	○	○	○	-	Length
	Tien & Chung(1979) : Eq.(3)	○	○	○	-	λ
	Prenger(1984) : Eq.(4)	○	-	○	-	h
	Ishii & Grolmes(1975) : Turbulent Eq.(7)	○	○	○	○	h
	Ishii & Grolmes(1975) : Turbulent Eq.(9)	○	○	○	○	λ d_1
Shear-induced	Cotter(1967) : Eq.(12)	○	-	○	-	h
	Kemme(1976) : Eq.(13)	○	-	○	-	d_1
	Chi(1976) : Eq.(15)	○	-	○	-	d_1
	Tien&Chung(1979) : Eq.(16)	○	○	○	-	d_1
	Prenger & Kemme (1981) : Eq.(17)	○	-	○	-	d_2
	Prenger(1984) : Eq.(19)	○	○	○	-	d_2
	Rice & Fulford(1987) : Eq.(20)	○	-	○	-	d_1

Note
1. The symbol, o, indicates that the corresponding parameter is included in the model.
2. h and λ_c represent the film thickness and the critical wave length, respectively
3. d_1 and d_2 are the wire spacing and the thickness of screen meshes, respectively.

A film thickness, h, of 4 mm was used as a characteristic dimension for the calculations of the wave-induced entrainment group, and the wire spacing for 40×40 copper mesh was utilized for that of the shear-induced entrainment group. Particularly, the hydraulic diameter, $d_{h,w}$, in equation(15) (Chi, 1976) was assumed to be the wire spacing, d_1, of the meshes, and wire thickness was used for the characteristic dimension, δ in equations (17) (Prenger and Kemme, 1981) and (19) (Prenger, 1984). The hydraulic diameter of the vapor core D_h was assumed to be 15.2 mm and 19.2 mm for the wave-induced and shear-induced entrainment, respectively.

The Critical Weber Number

In Fig. 5, the critical Weber number, e_{vc}, is plotted as a function of the viscosity number, N_{vi}, corresponding to the vapor(or saturation) temperature to show individual trends of the various models. The solid and blank symbols are associated with the wave-induced and shear-induced models, respectively. Six models including Cotter(1967) and Chi(1976) show that the critical Weber number remains unchanged

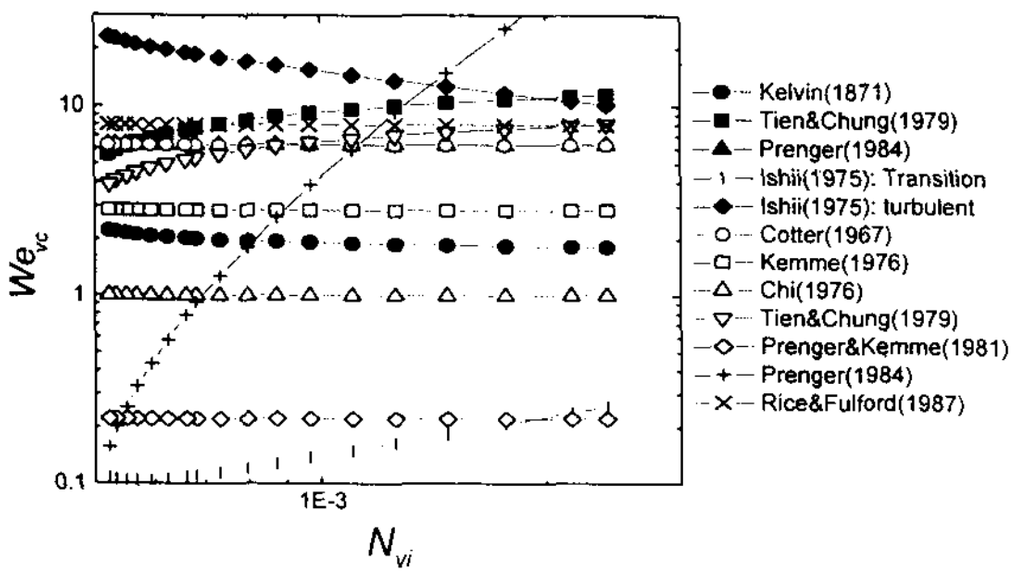

Fig. 5. The critical Weber number versus vapor temperature for various entrainment models

with decreases in the viscosity number. However, increasing trends are observed by the two models, the instability model for the wave-induced entrainment(Kelvin, 1871) and the turbulent roll-wave model (Ishii and Grolmes, 1975). Instead, decreasing trends are identified by the four models including Tien and Chung (1979) and Prenger (1984).

The overall trend shows that the order of magnitude of the critical Weber number varies from 0.1 to 20, and individual trends are not consistent with respect to the vapor temperature change. Model comparisons between Ishii and Grolmes (1975) and Prenger (1984) (for the shear-induced model) show significant discrepancies in their trends. In general, the critical Weber number tends to increase very rapidly with increases in the viscosity number for large values of the viscosity number, but the dependency diminishes as the viscosity number decreases, thereafter the Weber number approaches a limiting value according to Hinze (1955). In this sense, the theoretical shear-induced model presented by Prenger (1984) seems to lack theoretical validity. This may be caused by the inappropriate geometry, i.e., the configuration of the interface shown in Fig. 2 is appropriate for the wave-induced entrainment but not for the shear-induced entrainment. Also, the overall trend indicates that in most cases, the critical Weber does not show significant variations except for $N_{vi} < 0.0007$ regardless of the large difference in the predicted values.

The Critical Heat Transport

In Fig. 6, the entrainment limit is plotted as

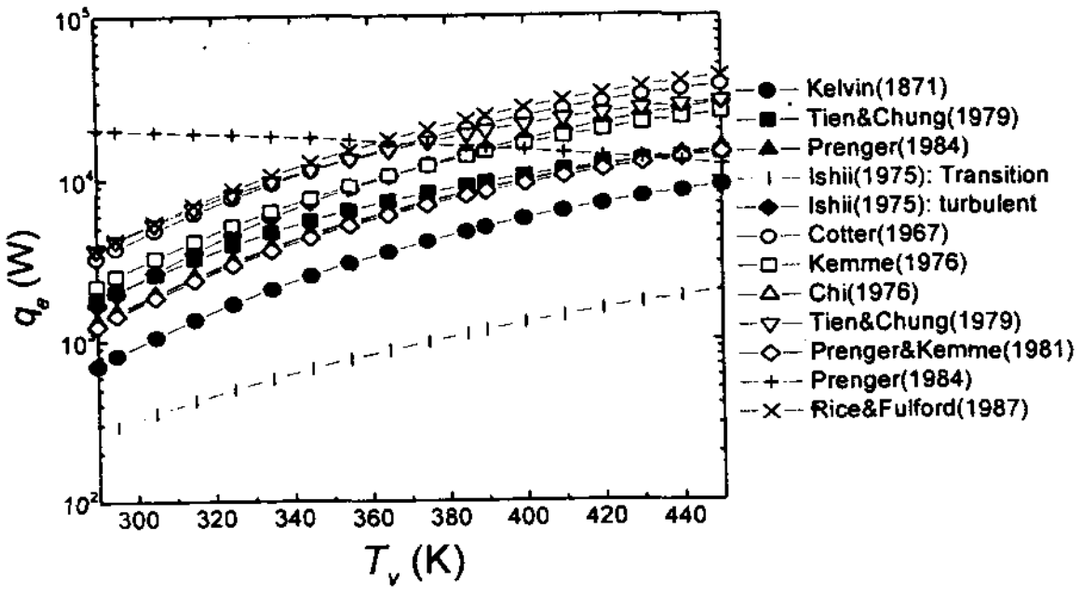

Fig. 6. Entrainment limit versus vapor temperature for various entrainment models

function of the vapor temperature to predict the individual and overall trends of the various models. The predicted entrainment limits vary from 0.3 kW at 290 K to about 30 kW at 490 K. It is evident that all the models show increasing trends in their entrainment limits with increases in the vapor temperature except the shear-induced model by Prenger (1984), which turns out to be less reasonable in its trend with respect to the viscosity number.

The increasing trends may be contradictory to the fact that the interface becomes more susceptible to increases in the vapor temperature due to the decrease in the viscosity number, as noted earlier. However, those trends can be explained by the significant increase in the vapor density as the operating temperature goes up. The vapor density of a saturated water at 450 K is about 360 times greater than at 290 K. This increase in the vapor density causes significant reductions in the vaporization rate, which results in decreases in vapor velocity. Therefore, more heat is required to maintain the vapor velocity above or equal to the

critical velocity for a given vapor temperature. In addition, the shear-induced entrainment models show larger entrainment limits than the wave-induced entrainment according to the overall trend since the wave-induced entrainment models have smaller vapor velocities when compared to the shear-induced entrainment. Particularly, the shear-induced model presented by Rice and Fulford(1987) predicts the largest entrainment limit, while the smallest value of the entrainment is obtained by the semi-empirical model of Prenger and Kemme(1981). For the wave-induced entrainment models, the lowest entrainment limit is predicted by the transition roll-wave model(Ishii and Grolmes, 1975). Also, the largest entrainment limit is obtained by the turbulent roll-wave model. These comparisions indicate variation ranging from a factor of ten for the wave-induced entrainment to four for the shear-induced entrainment.

CONCLUSIONS

Various entrainment or critical velocity models to predict stability of the wicked interface in operating heat pipes were examined to investigate individual trends and their discrepancies from the general trend. In order to organize the previous studies, twelve models were selected and categorized in two groups according to their entrainment mechanism, i.e., the wave-induced entrainment and the shear-induced entrainment.

For this purpose, critical Weber numbers and entrainment limits were calculated as a function of the vapor temperature for the given characteristic dimensions of the interface. The critical Weber number was presented in Fig. 5 as a function of the viscosity number. The overall trend shows that the order of magnitude of the critical Weber number varies from 0.1 to 20, and individual trends are not consistent with respect to the vapor temperature change. For the entrainment limit shown in Fig. 6, it is evident that the models show increasing trends in their entrainment limits as the vapor temperature increases, but these comparisions indicate variation ranging from a factor of ten for the wave-induced entrainment to four for the shear-induced entrainment. Although many of the analytical models predict entrainment from the capillary wick, it is necessary to conduct a combined analytical and experimental investigation because entrainment phenomena in operating heat pipes has not well understood yet.

REFERENCES

1. Busse, C. A., 1973, "Theory of the Ultimate Heat Transfer Limit of Cylindrical Heat Pipes," *International Journal of Heat Mass Transfer*, Vol. 16, p.169.
2. Busse, C. A. and Kemme, J. E., 1980, "Dry-out Phenomena in Gravity-Assisted Heat Pipes with Capillary Flow," *International Journal of Heat Mass Transfer*, Vol. 23, pp.634~654.
3. Carey, V. P., 1992, *Liquid-Vapor Phase*

Change Phenomena, Hemisphere Publishing Co., Washington, D. C., pp.90~98, 439~448.

4. Chi, S. W., 1976, *Heat Pipe Theory and Practice*, Hemisphere Publishing Co., Washington, D. C., pp.33~95.
5. Cotter, T. P., 1967, "Heat Pipe Startup Dynamics," *Proceedings of the SAE Thermionic Conversion Specialist Conference*, Palo Alto, California, October, pp.344~347.
6. Dobran, F., 1985, "Steady-State Characteristics and Stability Thresholds of a Closed Two-Phase Thermosyphons," *International Journal of Heat Mass Transfer*, Vol. 28, pp.949~957.
7. Drazin, P. G. and Reid, W. H., 1981, *Hydrodynamic Stability*, Cambridge University Press, Cambridge, United Kingdom, pp.14~22, 124~134.
8. Grover, G. M., Cotter, T. P. and Erickson, G. F., 1964, "Structures of Very High Thermal Conductivity," *J. Appl. Phys.*, Vol. 218, pp.1190~1191
9. Hinze, J. O., 1955, "Fundamentals of the Hydrodynamic Mechanism of Splitting in Dispersion Process," *AIChE J.*, Vol. 1, pp.289~295.
10. Ishii, M. and Grolmes, M.A., 1975, "Inception Criteria for Droplet Entrainment in Two-Phase Concurrent Film Flow," *AIChE J.*, Vol. 21, pp.308~318.
11. Ivanovskii, M. N., Sorokin, V. P. and Yagodkin, I. V., 1982, *The Physical Principles of Heat Pipe*, Clarendon Press, Oxford, United Kingdom, pp.107~115.
12. Kelvin, Lord, 1871, "Hydrokinetic solutions and observations," *Phil. Mag.*, Vol. 10, pp.155~168.
13. Kemme, J. E., 1976, "Vapor Flow Consideration in Conventional and Gravity Assisted Heat Pipes," *Proceedings of the 2nd Int'l. Heat Pipe Conference*, Bologna, Italy, March, pp.11~21.
14. Kim, B. H., Peterson, G. P. and Kihm, K. D., 1993, "Analytical and Experimental Investigation of Entrainment in Capillary-Pumped Wicking Structures," *Transactions of ASME Journal of Energy Resources and Technology*, Vol. 115, pp.278~286.
15. Kutateladze, S. S. and Sorokin, Y. L., 1969, "The Hydrodynamic Stability of Vapor-Liquid Systems," *Problems of Heat Transfer and Hydraulics of Two-Phase Media*, Pergamon Press, New York, pp.385~395.
16. Matveev, V. M., Filippov, Y. N., Dyuzhev, V. I. and Okhapkin, E. V., 1977, "Breakaway of a Liquid by a Gas Stream at an Interface Containing Grid," *Journal of Engineering Physics*, Vol. 33, No. 3, pp. 1008~1012.
17. Olson, R. M. and Eckert, E. R. G., 1966, "Experimental Studies of Turbulent Flow in a Porous Circular Tube with Uniform Fluid Injection through the Tube Wall," *Transactions of ASME, J. Applied Mechanics*, Ser. E, Vol. 33, No. 1.
18. Prenger, F. C., 1984, "Performance Limits of Gravity-Assisted Heat Pipes," *Proceedings of The 5th International Heat Pipe Conference*, Tsukuba, Japan, May, pp.137~146.
19. Prenger, F. C. and Kemme, J. E., 1981,

"Performance Limits of GravityAssisted Heat Pipes with Simple Wick Structures," *Proceedings of The 4th International Heat Pipe Conference*, London, United Kingdom, September, pp.137~146.

20. Rice, G. and Fulford, D., 1987, "Influence of a Fine Mesh Screen on Entrainment in Heat Pipes," *Proceedings of The 6th International Heat Pipe Conference*, Grenoble, France, May, pp.168~172.
21. Tien, C. L. and Chung, K. S., 1979, "Entrainment Limits in Heat Pipes," *AIAA Journal*, Vol. 17, No. 6, pp.230~238.
22. Wallis, G. B., 1969, *One Dimensional Two Phase Flow*, McGrawHill, New York, pp. 345~351 and 376~391.

Review of Entrainment and Interfacial Stability in Thermosyphons and Capillary-Driven Heat Pipes

B. H. Kim*, C. J. Kim**

* *Taegu University*

** *Sung Kyun Kwan University*

Abstract

Entrainment in thermosyphons and heat pipes was characterized in view of the interfacial stability associated with the critical Weber number and the entrainment limit at the onset of liquid entrainment from the liquid or wicked interface. Both literature review and theoretical analysis on the entrainment models were performed in order to evaluate accuracy of the predicted value.

For this purpose, the models were categorized in two groups according to their entrainment mechanism and interfacial configurations, i.e., the wave-induced entrainment and the shear-induced entrainment, respectively. Thus, the twelve models (five models for the wave-induced entrainment and seven for the shear induced entrainment) were examined to obtain individual trends and their discrepancies from the general tendency of the overall models. As a result, the critical Weber numbers and entrainment limits were calculated and represented as a function of vapor temperature for the chosen characteristic dimensions of the interface.